Active cathepsins B, L, and S in murine and human pancreatitis

Victoria Lyo, Fiore Cattaruzza, Tyson N. Kim, Austin W. Walker, Margot Paulick, Daniel Cox, Jordan Cloyd, James Buxbaum, James Ostroff, Matthew Bogyo, Eileen F. Grady, Nigel W. Bunnett and Kimberly S. Kirkwood

Am J Physiol Gastrointest Liver Physiol 303:G894-G903, 2012. First published 16 August 2012; doi:10.1152/ajpgi.00073.2012

Am J Physiol Gastrointest Liver Physiol 303: G894–G903, 2012.
First published August 16, 2012; doi:10.1152/ajpgi.00073.2012.

Active cathepsins B, L, and S in murine and human pancreatitis

Victoria Lyo,[1] Fiore Cattaruzza,[1] Tyson N. Kim,[1] Austin W. Walker,[1] Margot Paulick,[2] Daniel Cox,[1] Jordan Cloyd,[1] James Buxbaum,[3] James Ostroff,[3] Matthew Bogyo,[2] Eileen F. Grady,[1] Nigel W. Bunnett,[3] and Kimberly S. Kirkwood[1]

[1]*Department of Surgery, University of California, San Francisco, San Francisco, California;* [2]*Department of Pathology, Stanford University, Stanford, California;* [3]*Department of Gastroenterology, University of California, San Francisco, San Francisco, California; Departments of Pharmacology and Medicine, Monash Institute of Pharmaceutical Sciences, Parkville, Victoria, Australia*

Submitted 28 February 2012; accepted in final form 18 July 2012

Lyo V, Cattaruzza F, Kim TN, Walker AW, Paulick M, Cox D, Cloyd J, Buxbaum J, Ostroff J, Bogyo M, Grady EF, Bunnett NW, Kirkwood KS. Active cathepsins B, L, and S in murine and human pancreatitis. *Am J Physiol Gastrointest Liver Physiol* 303: G894–G903, 2012. First published August 16, 2012; doi:10.1152/ajpgi.00073.2012.— Cathepsins regulate premature trypsinogen activation within acinar cells, a key initial step in pancreatitis. The identity, origin, and causative roles of activated cathepsins in pancreatic inflammation and pain are not defined. By using a near infrared-labeled activity-based probe (GB123) that covalently modifies active cathepsins, we localized and identified activated cathepsins in mice with cerulein-induced pancreatitis and in pancreatic juice from patients with chronic pancreatitis. We used inhibitors of activated cathepsins to define their causative role in pancreatic inflammation and pain. After GB123 administration to mice with pancreatitis, reflectance and confocal imaging showed significant accumulation of the probe in inflamed pancreas compared with controls, particularly in acinar cells and macrophages, and in spinal cord microglia and neurons. Biochemical analysis of pancreatic extracts identified them as cathepsins B, L, and S (Cat-B, Cat-L, and Cat-S, respectively). These active cathepsins were also identified in pancreatic juice from patients with chronic pancreatitis undergoing an endoscopic procedure for the treatment of pain, indicating cathepsin secretion. The cathepsin inhibitor K11777 suppressed cerulein-induced activation of Cat-B, Cat-L, and Cat-S in the pancreas and ameliorated pancreatic inflammation, nocifensive behavior, and activation of spinal nociceptive neurons. Thus pancreatitis is associated with an increase in the active forms of the proteases Cat-B, Cat-L, and Cat-S in pancreatic acinar cells and macrophages, and in spinal neurons and microglial cells. Inhibition of cathepsin activation ameliorated pancreatic inflammation and pain. Activity-based probes permit identification of proteases that are predictive biomarkers of disease progression and response to therapy and may be useful noninvasive tools for the detection of pancreatic inflammation.

experimental acute pancreatitis; pain; cathepsins; activity-based probes; near-infrared imaging

PREMATURE ACTIVATION OF TRYPSINOGEN is critical to the initiation of pancreatitis. Cysteine cathepsins (Cat) control trypsinogen processing within acinar cells and contribute to the development of pancreatitis (5, 13, 29, 35). Our understanding of these events has been limited by difficulties in isolating and measuring active forms of proteases in tissue. This limitation has, in turn, hindered efforts to delineate the pathways by which activated proteases cause pain, which is a major clinical problem in patients with both acute and chronic forms of pancreatitis.

Proteases control inflammation and pain by generating mediators and cleaving protease-activated receptors. Proteases are particularly important in pancreatitis, an autodigestive disease in which prematurely activated digestive enzymes, such as trypsin, cause pancreatic injury, inflammation, and pain. Proteases from infiltrating inflammatory cells and the circulation may also contribute to pancreatitis. However, the identity and cellular source of the proteases that are activated in pancreatitis are unknown, and their causative roles in pancreatic inflammation and pain are incompletely defined.

Cysteine cathepsins, of which there are 11 in the human genome, have diverse pathophysiological functions (5). By degrading proteins in acidified organelles, cathepsins regulate protein turnover, zymogen activation, antigen presentation, and hormone processing. Cathepsins play important roles in cancers, osteoporosis, inflammatory/immune diseases, and allergic disorders. Cathepsins contribute to pancreatitis by regulating the activity of trypsin within acinar cells. Cathepsin B (Cat-B) mediates the premature and inappropriate activation of trypsinogen, an important early event in the pathogenesis of pancreatitis since Cat-B inhibition or deletion attenuates trypsinogen activation and pancreatic inflammation (13, 29, 35). Cathepsin L (Cat-L) can degrade both trypsinogen and trypsin and could thereby mitigate the harmful effects of Cat-B by reducing trypsin activity (36). However, Cat-L deletion lessens the severity of pancreatic inflammation (36), suggesting a more complex role for Cat-L, possibly involving induction of apoptosis. In addition to their intracellular roles, certain cathepsins are also secreted and can remain fully [cathepsin S (Cat-S)] or partially (Cat-B, Cat-L) active in the extracellular environment, where they may have widespread effects (28). Cat-S is secreted by spinal microglia after neuronal injury and is critical for maintenance of neuropathic pain (8, 9).

Analysis of nucleic acid or protein expression fails to provide information on dynamic, posttranslational regulation and activity levels of enzymatic proteins such as proteases. Pancreatic proteases are synthesized as inactive zymogens and, once activated, participate in complex enzymatic cascades and are also subject to tight posttranslational regulation by endogenous inhibitors. Thus, to accurately determine the impact of proteases, we need to measure functional activity within a diseased tissue. However, conventional activity assays are limited by lack of selectivity and are unsuited for dynamic determination of protease activity in intact organisms. Activity-based probes (ABPs) are small molecule probes that can be used to localize and identify proteases in their active forms

Address for reprint requests and other correspondence: K. S. Kirkwood, UCSF, 513 Parnassus Ave., Rm. S1268, San Francisco, CA 94143-0660 (e-mail: kim.kirkwood@ucsfmedctr.org).

(10). ABPs comprise a warhead group, usually derived from a protease inhibitor, that covalently binds to the active site, plus a peptide linker, and a near-infrared tag for detection. When administered to experimental animals, ABPs can be used to monitor protease activity in diseased organs in vivo, and even in situ. Probe-bound proteases can be subsequently localized at the cellular level, and identified by proteomic analysis. ABPs based on an acyloxymethylketone warhead have been used to localize and identify active cathepsins in tumors (3, 4) but have not been used to study cathepsins in inflammatory diseases such as pancreatitis.

We used ABPs with an acyloxymethylketone warhead and a near-infrared tag to identify and localize active forms of cathepsins in the pancreas and spinal cord during pancreatitis. By reflectance imaging and two-photon confocal microscopy of intact organs, we detected active cathepsins throughout the pancreas and in the thoracic spinal cord from mice with acute pancreatitis. Active cathepsins were localized to acinar cells and infiltrating macrophages of the pancreas, and to spinal microglial cells and neurons. Proteomic analysis revealed a marked increase in active forms of Cat-B, Cat-L, and Cat-S in the inflamed mouse pancreas and in pancreatic juice from patients with chronic pancreatitis. Cathepsin inhibition ameliorated pancreatic inflammation and pain in mice. We identified increased active forms of Cat-B and Cat-L in acinar cell lysosomes and increased active Cat-S in macrophages of the pancreas and spinal cord. Our data support the notion that active cathepsins are essential for pancreatic inflammation and pain and secreted cathepsins could contribute to human pancreatitis pain. Moreover, ABPs can be used to identify biomarkers of disease progression and response to therapy.

MATERIALS AND METHODS

Mice. The University of California, San Francisco (UCSF) Institutional Animal Care and Use Committee approved all procedures with mice. C57BL/6 mice (male, female, 20–25 g) were from Charles River Laboratories (Hollister, CA). Mice were maintained under temperature- (22 ± 4°C) and light- (12-h light-dark cycle) controlled conditions with free access to food and water. Mice were killed with sodium pentobarbital (200 mg/kg ip).

Materials. GB123, a nonquenched ABP with an acyloxymethylketone warhead and a Cy5.5 tag, has been described (Fig. 1*A*) (3, 4). GB123 interacts with cysteine cathepsins and is serum stable, cell permeant, and suitable for administration to animals. Human Cat-B, Cat-L, and Cat-S were from EMD Biosciences (La Jolla, CA). K11777 (17) (Fig. 1*B*) was a gift from Dr. J. McKerrow (UCSF), and HALT Complete Protease Inhibitor Cocktail was from Pierce (Rockford, IL). Sources of primary antibodies are shown in Table 1. Biotinylated anti-rabbit IgG was from Vector Laboratories (Burlingame, CA). Anti-IgG conjugated to Rhodamine RedX was from Jackson Immunoresearch (West Grove, PA). Other reagents were from Sigma-Aldrich (St. Louis, MO).

Cerulein-induced pancreatitis and administration of ABP. Mice received hourly injections of cerulein (50 μg/kg ip) or vehicle (0.9% NaCl) for 12 h (6). A subset of mice was treated with K11777 (50 mg/kg ip) or vehicle (30% DMSO H_2O) twice daily starting 1 day prior to induction of pancreatitis and continuing throughout the experiment. Mice either were killed immediately after the final dose of cerulein or received GB123 (25 nmol/mouse, 66% DMSO PBS, 100 μl iv) 30 min after the final cerulein dose and were killed 24 h later. Some mice received GB123 intrathecally (1.25 nmol/mouse, 66% DMSO PBS, 10 μl) after the tenth cerulein dose, and the spinal cord was collected after the final dose of cerulein. Mice were transcardially perfused with 30 ml 0.1 M PBS pH 7.4 and tissues were collected for analysis.

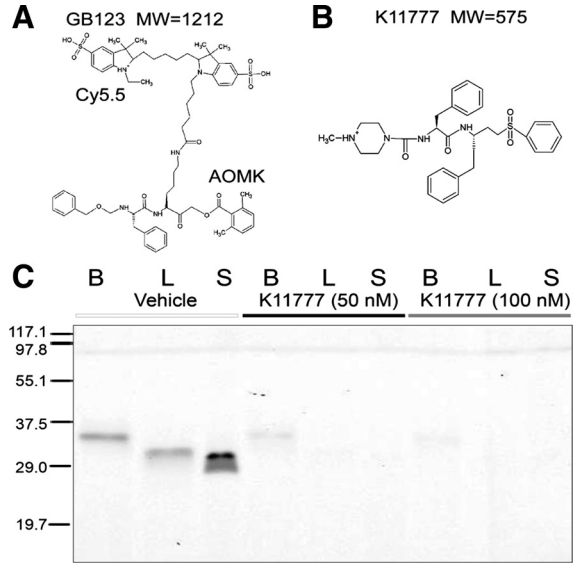

Fig. 1. GB123 interacts with purified cathepsins. *A*: GB123 with a Cy5.5 fluorophore and an acyloxymethylketone (AOMK) warhead that binds to the active site of cysteine cathepsins. MW, molecular weight. *B*: K11777, an irreversible cathepsin inhibitor. *C*: human cathepsin B (Cat-B), cathepsin L (Cat-L), or cathepsin S (Cat-S) (25 ng) (B, L, and S, respectively) were bound to GB123. Probe-bound proteases were detected by SDS-PAGE and in-gel fluorescence. K11777 (50–100 nM) abolished GB123 binding.

Ex vivo reflectance imaging of the pancreas. Excised pancreata were analyzed for GB123 by reflectance imaging (Xenogen IVIS100, Caliper Life Sciences, Hopkinton, MA) using the Cy5.5 filter. Signals from cerulein-treated pancreata were normalized to signals in control pancreata in each experimental group and are expressed as fold increase over control.

Two-photon imaging of pancreas and spinal cord. Pancreas and spinal cord (T8–T9) were fixed in 4% paraformaldehyde 0.1 M PBS pH 7.4 (1 h, room temperature), and optically cleared in a gradient of 5–60% sucrose PBS. Flat-mounted tissues in 60% sucrose were imaged by use of a locally designed two-photon laser scanning microscope. Low-energy 100-fs 80-MHz pulses were generated by use of a titanium-sapphire laser oscillator (Mai Tai, Newport Spectra-Physics, Irvine, CA) tuned to 1,020 nm for excitation of Cy5.5. MPScan imaging software was used to control the microscope and collect images (24). Stacks of images (400 μm deep at 1-μm axial spacing) were collected and analyzed with Image J (NIH). Identical collection parameters were used for pancreatitis and control tissues.

Immunofluorescence confocal imaging of pancreas and spinal cord. Pancreas and spinal cord (T8–T9) were fixed in paraformaldehyde (4 h, room temperature), cryoprotected (30% sucrose PBS, overnight, 4°C), and frozen sections (10–14 μm) were prepared. Sections were incubated with primary antibodies (Table 1) in 0.1 M PBS pH 7.4, 10% normal horse serum, and 0.1% Triton X-100. Sections were incubated with fluorescent secondary antibodies (1:200, 1 h, room temperature). Sections were observed by using a Zeiss LSM510 Meta and Axiovert microscope with Plan Neo-Fluar ×40 (NA 0.8) and Plan Neo-Fluar ×63 (NA 1.4) objectives. Images (1,024 × 1,024 pixels) were acquired at 0.44- to 0.74-μm intervals by using a pinhole of 1.04–1.86 Airy units. Identical collection parameters were used for pancreatitis and control tissues.

Human pancreatic juice. Human pancreatic juice was obtained from patients with chronic pancreatitis undergoing endoscopic retrograde cholangiopancreatography. The protocol was approved by the UCSF Human Subjects Committee, and samples were collected with

Table 1. *Primary antibodies*

Antibody	Species	Conditions	Source
Mouse Cat-B (AF965)	Goat	IP: 1.0 μg, overnight, 4°C	R&D Systems (Minneapolis, MN)
Mouse Cat-L (AF1515)	Goat	IP: 1.0 μg, overnight, 4°C	R&D Systems (Minneapolis, MN)
Human Cat-S (AF1183)	Goat	IP: 1.0 μg, overnight, 4°C	R&D Systems (Minneapolis, MN)
Cat-B (S-12 sc-6493)	Goat	IF: 1:300, overnight, 4°C	Santa Cruz Biotechnology (Santa Cruz, CA)
Cat-L (D-20 sc-6501)	Goat	IF: 1:300, overnight, 4°C	Santa Cruz Biotechnology (Santa Cruz, CA)
Cat-S (M-19 sc-6505)	Goat	IF: 1:300, overnight, 4°C	Santa Cruz Biotechnology (Santa Cruz, CA)
F4/80	Rat	IF: 1:200, overnight, 4°C	BMA Biomedicals (Augst, Switzerland)
LAMP1	Rat	IF: 1:300, overnight, 4°C	ABR Affinity Bioreagents (Golden, CO)
NeuN	Mouse	IF: 1:500, overnight, 4°C	Millipore (Billerica, MA)
GFAP (AB5541)	Chicken	IF: 1:250, overnight, 4°C	Millipore (Billerica, MA)
Ox42 (M1/70)	Rat	IF: 1:200, overnight, 4°C	BD Pharmigen (San Diego, CA)
β-Actin	Mouse	WB: 1:10,000, overnight, 4°C	Sigma-Aldrich (St. Louis, MO)
c-Fos	Rabbit	IH: 1:20,000, overnight, 4°C	Chemicon (Temecula, CA)

IF, immunofluorescence; IH, immunohistochemistry; WB, Western blotting; IP, immunoprecipitation.

informed patient consent. Aliquots were either immediately frozen in liquid nitrogen or pretreated with K11777 (50 nM) or HALT protease inhibitor cocktail (1×) with 5 mM EDTA before freezing.

In vitro reactions with ABPs. Human Cat-B, Cat-L, or Cat-S (25 ng) was incubated with K11777 (50 or 100 nM) or vehicle (30% DMSO in H_2O) for 30 min at room temperature in 400 mM sodium acetate pH 5.5, 4 mM EDTA, 8 mM DTT (Cat-B, Cat-L) or 20 mM potassium phosphate pH 7.4, 5 mM EDTA, 5 mM DTT (Cat-S). GB123 was added (1 μM final) and allowed to react for 1 h. Human pancreatic juice (20 μg protein) was similarly incubated with K11777 (50 nM), HALT (1×) or vehicle and GB123. Reactions were stopped by boiling (5 min) in 4 × sample buffer (200 mM Tris pH 6.8, 12% SDS, 40% glycerol, 0.4 mg/ml bromophenol blue, 5% β-mercaptoethanol). Samples were analyzed by SDS-PAGE (15% acrylamide), and GB123-bound proteins were detected by in-gel fluorescence (700 nm; Odyssey Infrared Imaging System, LiCOR Bioscience, Lincoln, NE).

SDS-PAGE and Western blotting. Pancreata from GB123-treated mice were homogenized in 5 mM MOPS pH 6.5, 250 mM sucrose. Homogenates (60 μg protein) were analyzed by SDS-PAGE and in-gel fluorescence. Proteins were transferred to polyvinylidene difluoride membranes, which were analyzed by Western blotting for β-actin. GB123 signals were normalized to β-actin signals, and signals from cerulein-treated samples were expressed as fold control.

Immunoprecipitation. Pancreas homogenates from GB123-treated mice (200 μg protein) or GB123-treated human pancreatic juice (50 μg protein) were incubated with antibodies to Cat-B, Cat-L, or Cat-S [1–2 μg, 0.75 ml of RIPA buffer (50 mM Tris·HCl pH 7.4, 150 mM NaCl, 5 mM EDTA, 0.5% deoxycholate, 0.1% SDS), 1 h, room temperature]. Protein A/G Plus Agarose beads (Santa Cruz Biotechnology) were added and incubated overnight at 4°C. Beads were washed with RIPA and analyzed by SDS-PAGE and in-gel fluorescence.

Assessment of pancreatitis. Pancreatitis was assessed by measurement of serum amylase activity, wet pancreatic weight normalized to body weight, and histological examination (6). For histology, sections stained with hematoxylin and eosin were evaluated by an investigator unaware of the experimental groups and scored on a scale from 0–5 for *1*) macrolobular edema, *2*) microlobular edema, *3*) zymogen degranulation, *4*) polymorphonuclear leukocyte infiltration, *5*) polymorphonuclear leukocytes in peripancreatic fat, *6*) vacuoles in acinar

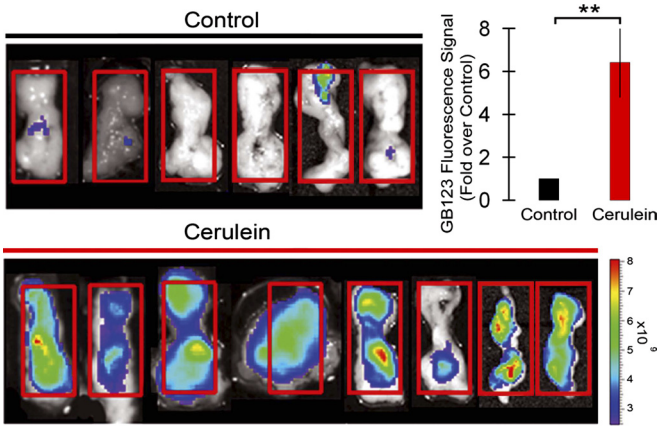

Fig. 2. Reflectance imaging of activated pancreatic cathepsins. Pancreas from GB123-treated mice show increased GB123 signal in cerulein-treated mice, determined by reflectance imaging [red box denotes region of interest from which signal was quantified; scale denotes photons per second per square centimeter per steradian ($p \cdot s^{-1} \cdot cm^{-2} \cdot sr^{-1}$)]. Fluorescence signal in cerulein-treated pancreata are expressed as fold control. Control, $n = 6$; cerulein, $n = 8$. $^{**}P < 0.01$.

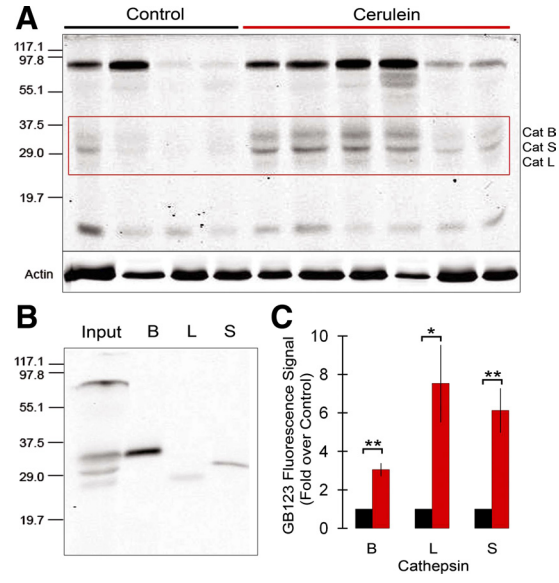

Fig. 3. Identification of activated pancreatic Cat-B, Cat-L, and Cat-S. *A*: pancreas homogenates from GB123-treated mice were analyzed by SDS-PAGE and in-gel fluorescence. GB123-bound proteases corresponding in mass to Cat-B, Cat-L, and Cat-S were activated after cerulein. Nonspecific proteins of ~10 kDa and 90 kDa also bound to GB123, as described (4). *B*: immunoprecipitation confirmed identify of Cat-B, Cat-L, and Cat-S. *C*: quantification revealed activation of Cat-B, Cat-L, and Cat-S. Control, $n = 4$; cerulein, $n = 6$. $^{*}P < 0.05$, $^{**}P < 0.01$.

cells, and *7*) necrosis. Scores were tabulated and the mean value for each experimental group defined the histological severity score.

Assessment of pancreatic pain. To assess activation of nociceptive spinal neurons, c-Fos-immunoreactivity (IR) was localized in sections (45 μm) of spinal cord (T6–T12) by immunohistochemistry (6). Slides were examined by an investigator unaware of the experimental groups. Fos-stained nuclei in laminae I/II of the spinal cord were counted in six to eight sections per animal with use of a ×20 objective, and mean data were determined for each mouse. Pancreatitis-associated pain was evaluated as described for assessment of visceral pain (6, 20, 31). After the last dose of cerulein, mice were videorecorded for 30 min. The number of abdominal retractions (including hunching), abdominal squashes, abdominal stretches, and abdominal licking events were recorded by two investigators unaware of the experimental treatments and were summed.

Statistical analysis. Results are expressed as means ± SE from $n \geq 6$ mice per group. Results were compared by Student's *t*-test (2 comparisons) or ANOVA (>2 comparisons) followed by Dunnett's multiple comparisons to one control. Histology severity scores (nonparametric data) were statistically assessed by using Kruskal-Wallis test and Dunn's multiple-comparisons posttest.

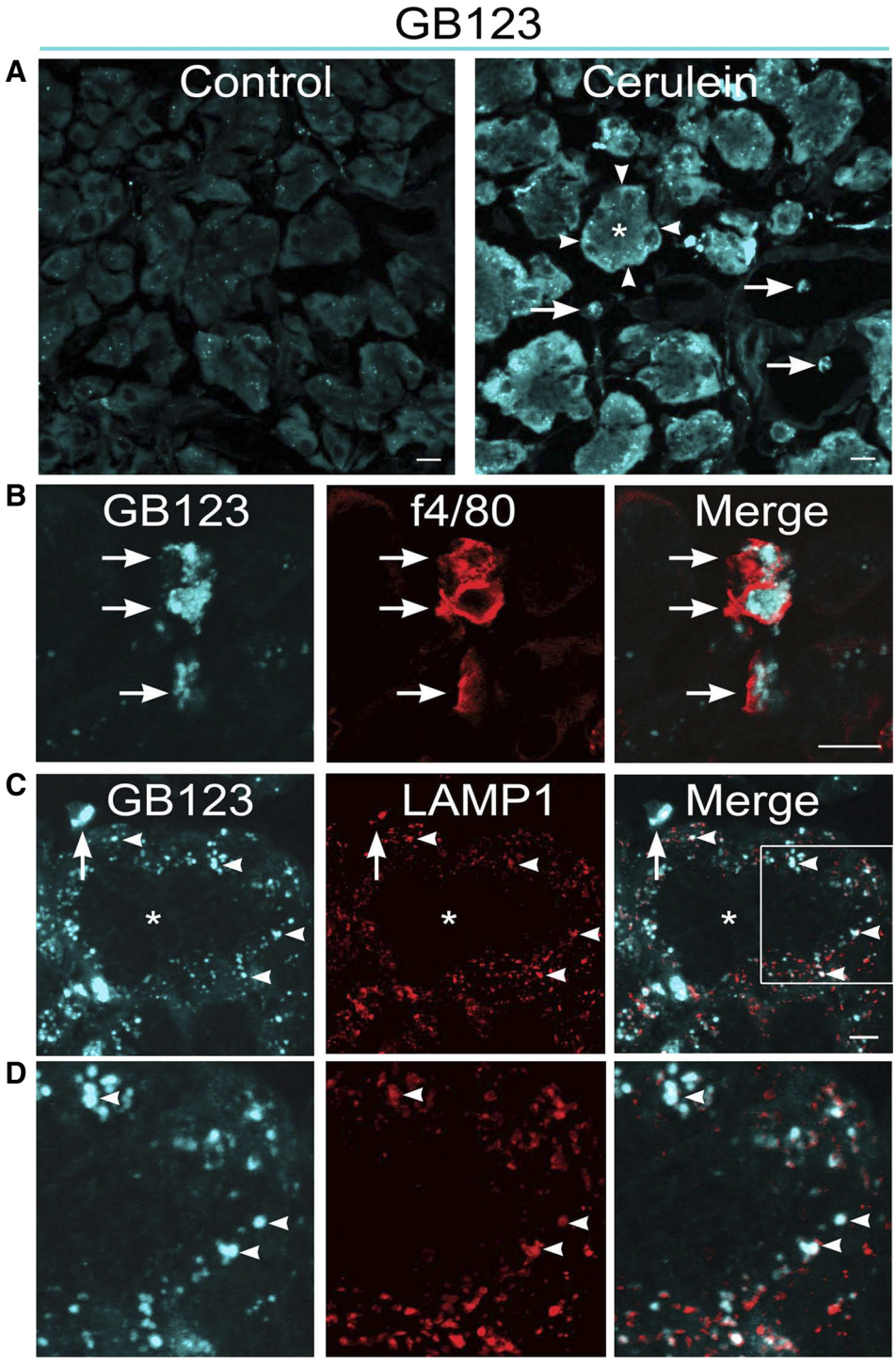

Fig. 4. Localization of activated cathepsins in pancreatic acinar cells and macrophages. *A*: confocal imaging of pancreata from GB123-treated mice revealed accumulation of GB123 in in acinar cells (arrowheads, *acinus lumen) and parenchymal infiltrating cells in cerulein-treated mice. *B*: GB123 colocalized with the macrophage marker f4/80. *C* and *D*: GB123 colocalized with the lysosomal marker LAMP1 within acinar cells (arrowheads). *D* is magnified view of box in *C*. Scale, 10 μm.

RESULTS

GB123 interacts with activated Cat-B, Cat-L, and Cat-S. GB123 is a nonquenched ABP with an acyloxymethylketone warhead and a Cy5.5 tag (Fig. 1*A*; Refs. 3, 4). GB123 interacts with cysteine cathepsins and is serum-stable, cell-permeant and suitable for administration to animals. To verify interaction with activated cathepsins, we incubated GB123 with human cathepsins and analyzed reactions by SDS-PAGE and in-gel Cy5.5 fluorescence. GB123 interacted with Cat-B, Cat-L, and Cat-S (Fig. 1*C*). To examine selectivity for active cathepsins, we preincubated proteases with K11777, an irreversible vinyl sulfone cathepsin inhibitor (Fig. 1*B*; Ref. 17). K11777 abolished the interaction between GB123 and Cat-B, Cat-L, and Cat-S (Fig. 1*C*), confirming the requirement for cathepsin activity.

Detection of activated cathepsins by reflectance imaging of the inflamed pancreas. To examine the activation of cathepsins in the inflamed pancreas, we administered GB123 to control mice and mice with pancreatitis induced by treatment with the secretagogue cerulein (6). After 24 h, when unbound GB123 was excreted, pancreata were removed and accumulation of GB123 was examined by reflectance imaging. GB123 fluorescence was 6.4-fold higher in the inflamed compared with the uninflamed pancreas ($P < 0.01$ to control) (Fig. 2), consistent with activation of cathepsins in the inflamed pancreas.

Identification of activated Cat-B, Cat-L, and Cat-S in the inflamed pancreas. Since GB123 covalently interacts with activated cathepsins, GB123-bound proteases can be fractionated by SDS-PAGE, detected by in-gel fluorescence, and identified immunochemically. Analysis of pancreatic homogenates from GB123-treated mice identified three fluorescent proteins with apparent molecular masses corresponding to cathepsins (Fig. 3*A*, red box), and a high-molecular-weight protein corresponding to an unidentified serum protein known to interact with GB123 (4). Immunoprecipitation confirmed the identity of Cat-B, Cat-L, and Cat-S in pancreas extracts (Fig.

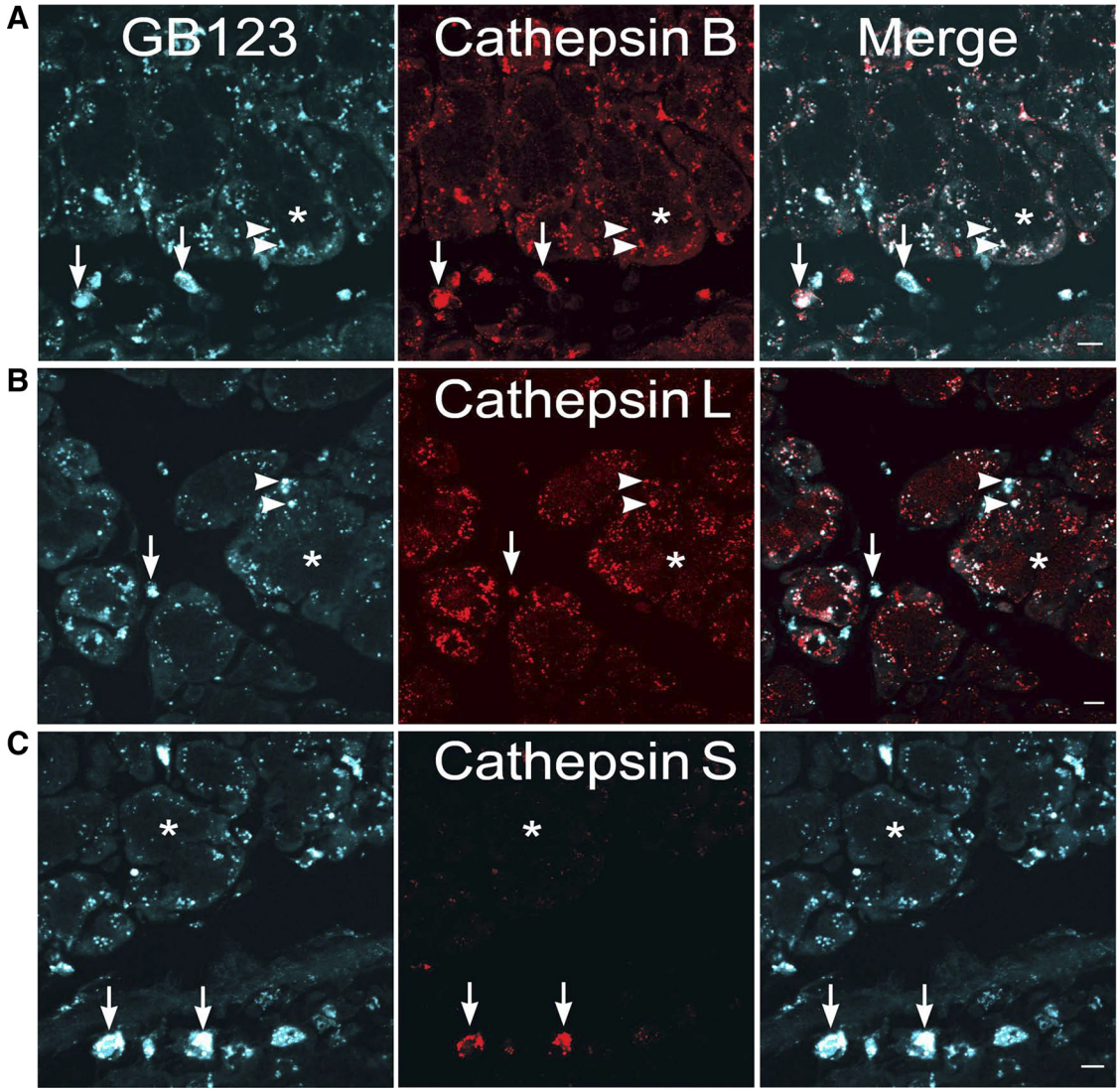

Fig. 5. Localization of pancreatic Cat-B, Cat-L, and Cat-S in the pancreas. Confocal imaging of pancreata from GB123-treated mice with cerulein pancreatitis revealed colocalization of GB123 with Cat-B-IR (*A*) and Cat-L-IR (*B*) in macrophages (arrows) and in lysosomes of acinar cells (arrows, *acinus lumen). GB123 colocalized with Cat-S-IR, which was restricted to macrophages (*C*, arrows). Scale, 10 μm.

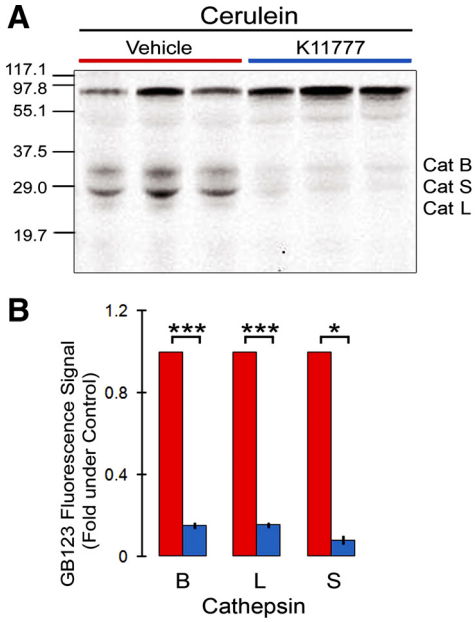

Fig. 6. K11777 inhibition of pancreatic cathepsins. Analysis of pancreatic extracts of GB123-treated mice with cerulein pancreatitis by SDS-PAGE and in-gel fluorescence indicated that systemic K11777 suppressed Cat-B, Cat-L, and Cat-S activity (*A*), which was confirmed by quantification (*B*). Vehicle, $n = 4$; K111777, $n = 6$. $^{*}P < 0.05$, $^{***}P < 0.001$.

3*B*). Quantification of GB123 signals revealed upregulation of Cat-B by 3.1-fold ($P < 0.01$), Cat-L by 7.5-fold ($P < 0.05$), and Cat-S by 6.1-fold ($P < 0.01$) in the inflamed pancreas compared with controls (Fig. 3*C*).

Cellular localization of activated cathepsins in the inflamed pancreas. Although previous studies of Cat-B and Cat-L in pancreatitis examined their role in processing trypsinogen within pancreatic acinar cells (13, 29, 35, 36), cathepsins are widely expressed in other cell types, including immune cells, which are known to infiltrate the inflamed pancreas. To confirm activation and to identify the cellular source of cathepsins, we localized GB123-bound proteases in the pancreas by confocal microscopy. Given the deep penetrance of near-infrared fluorophores, we used two-photon microscopy to collect stacks of optical sections (400 μm deep, 1-μm intervals), allowing localization of GB123 throughout the intact excised pancreas. This analysis, presented in video format, revealed a marked increase in the GB123 signal in the inflamed pancreas (Supplemental Fig. S1). GB123 fluorescence was increased throughout the entire depth and in all lobes of the pancreas and was localized to acinar cells and smaller infiltrating cells. Analysis of pancreatic sections by single-photon microscopy allowed characterization of the cellular and subcellular location of GB123. This analysis confirmed the increase in GB123 fluorescence in the pancreas from cerulein-treated mice and revealed probe accumulation in the basolateral region of acinar cells (Fig. 4*A*, arrowheads) and in infiltrating inflammatory cells within pancreatic vessels and in the parenchyma (Fig. 4*A*, arrows). Simultaneous localization of macrophages with use of antibodies to F4/80 indicated that GB123 was prominently localized to infiltrating macrophages (Fig. 4*B*). GB123 also colocalized with the lysosomal marker LAMP1 in acinar cells (Fig. 4, *C* and *D*, arrowheads) and macrophages (Fig. 4, *C* and *D*, arrow). Thus cathepsins are activated in macrophages and acinar cells of the inflamed pancreas.

Cellular localization of active Cat-B, Cat-L, and Cat-S in the inflamed pancreas. Since the GB123 fluorescence represents signals from at least three activated cathepsins, we colocalized GB123 with Cat-B-, Cat-L-, or Cat-S-IR. Cat-B-IR and Cat-L-IR colocalized with GB123 in lysosomes of acinar cells (Fig. 5, *A* and *B*, arrowheads) and macrophages (Fig. 5, *A* and *B*, arrows). However, Cat-S-IR was detected only in macrophages, where it colocalized with GB123 (Fig. 5*C*, arrows). These results are consistent with the reported limited expression of Cat-S in cells of mononuclear-phagocytic origin (25), whereas Cat-B and Cat-L are widely expressed (5).

Contributions of activated cathepsins to pancreatic inflammation and pain. To assess the causative role of cathepsins in pancreatitis and pancreatic pain, we treated mice with the cathepsin inhibitor K11777 or vehicle prior to cerulein administration. We also administered GB123 to verify effective inhibition of cathepsins within the pancreas. Analysis of pancreatic homogenates by electrophoresis and in-gel fluorescence showed that K11777 inhibited Cat-B by 6.7-fold, Cat-L by 6.5-fold, and Cat-S by 12.5-fold compared with vehicle (all $P < 0.05$), confirming effective inhibition of pancreatic cathepsins (Fig. 6). In a separate cohort of mice, we examined the effects of K11777 on inflammatory and pain end points. In mice treated with vehicle, cerulein caused increased serum amylase activity (Fig. 7*A*), pancreatic edema (pancreatic weight/total body, Fig. 7*B*), and total histological severity scores (Fig. 7*C*). K11777 reduced serum amylase by 1.49-fold, edema by 1.32-fold, and histological severity score by 1.53-fold (all $P < 0.05$ to vehicle). In particular, cathepsin inhibition reduced zymogen

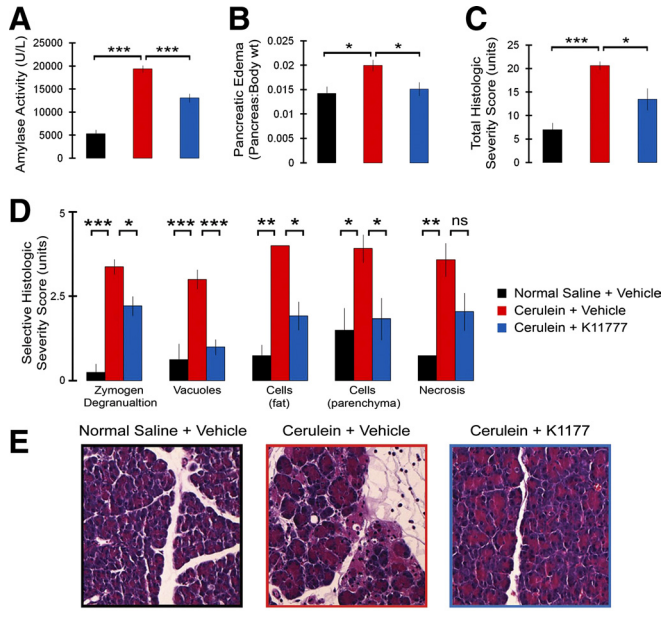

Fig. 7. K11777 inhibition of cerulein-induced pancreatic inflammation. Mice were treated with saline and vehicle (black, $n = 4$), cerulein and vehicle (red, $n = 6$) or cerulein and K11777 (blue, $n = 6$). Cerulein increased serum amylase (*A*), pancreatic edema (*B*) and histological severity score (*C*), including zymogen degranulation, vacuolarization, infiltration of inflammatory cells and necrosis (*D* and *E*). K11777 decreased all end points except for histological scoring of edema and hemorrhage. $^{*}P < 0.05$, $^{**}P < 0.01$. $^{***}P < 0.001$.

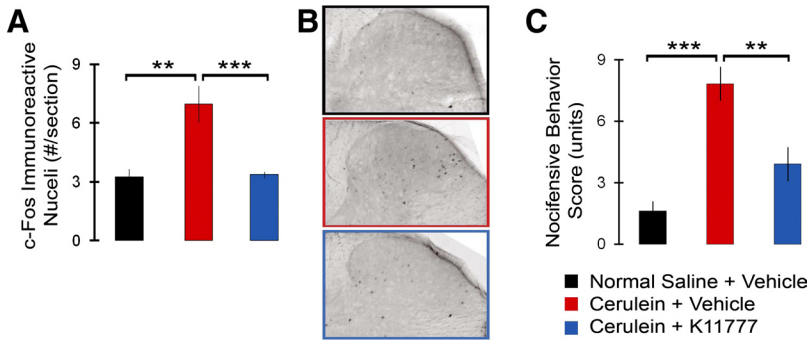

Fig. 8. K11777 inhibition of cerulein-induced pancreatitis pain. Mice were treated with saline and vehicle (black, $n = 4$), cerulein and vehicle (red, $n = 6$) or cerulein and K11777 (blue, $n = 6$). Cerulein increased the number of c-Fos-IR nuclei in the dorsal horn laminae I/II (*A* and *B*) and nocifensive behavior (*B*). K11777 significantly reduced cerulein-induced c-Fos-IR and nocifensive behaviors. $^{**}P < 0.01$, $^{***}P < 0.001$.

degranulation, vacuolization, infiltrating cells within peripancreatic fat and in the parenchyma, and necrosis, but it did not affect microscopic edema (Fig. 7*D*).

As previously reported, cerulein-induced pancreatitis increased the number of neurons expressing nuclear c-Fos-IR bilaterally in laminae I/II of the lower thoracic spinal cord (T8–T10), which receives afferent input from the pancreas (Fig. 8, *A* and *B*) (6). This finding is consistent with the activation of spinal nociceptors during pancreatitis. K11777 caused a 2.15-fold reduction in the number of neurons expressing c-Fos-IR ($P < 0.001$ to vehicle). To corroborate these findings, we quantified pain-related behavior. Cerulein-induced

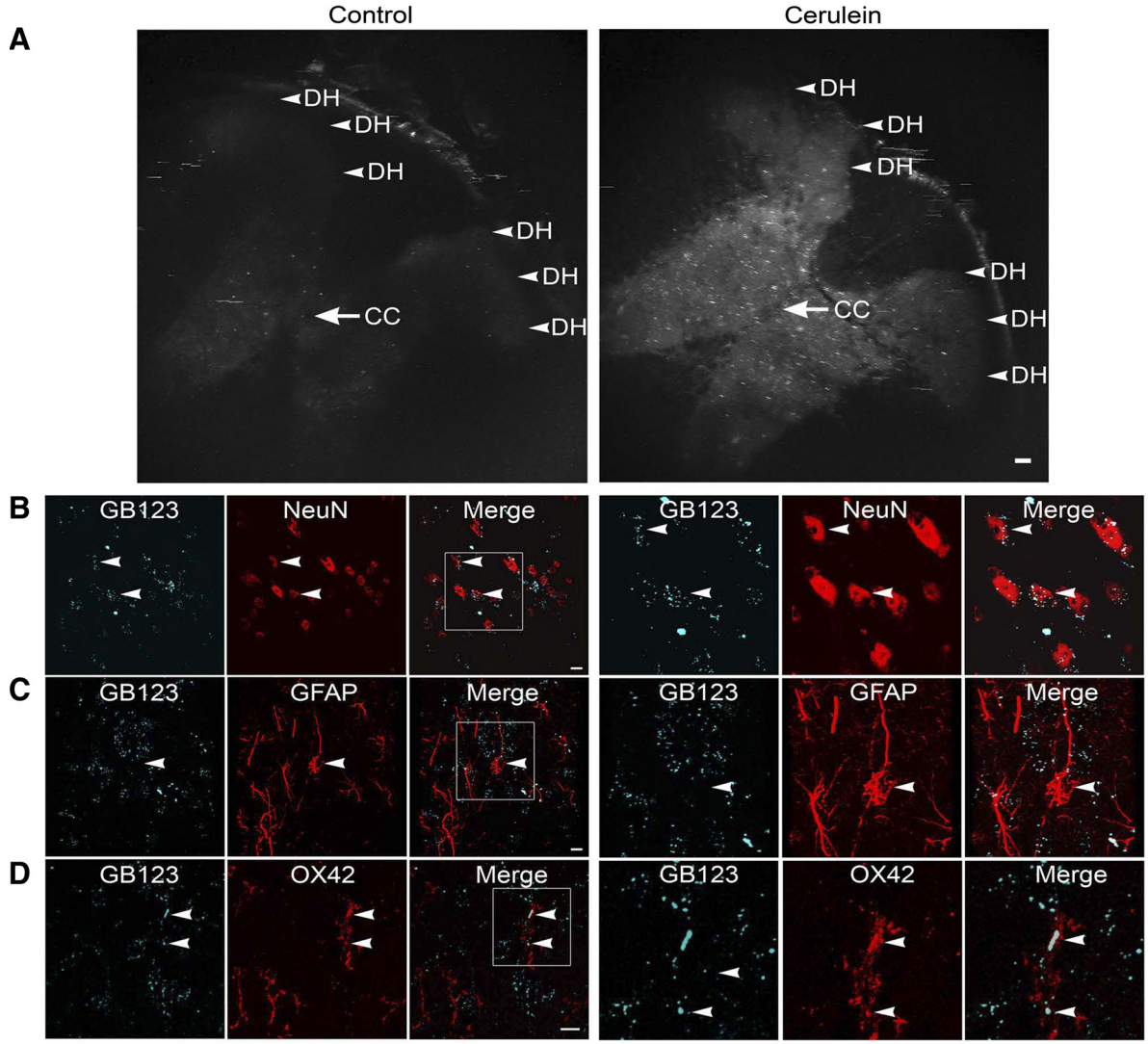

Fig. 9. Localization of activated cathepsins in the spinal cord of mice with pancreatitis. Mice received saline or cerulein followed by 1 intrathecal injection of GB123. *A*: 2-photon imaging of spinal cord (T8–T10) revealed GB123 accumulation throughout the dorsal horn in cerulein-treated mice. DH, dorsal horn; CC, central canal. *B* and *C*: single-photon imaging of sections revealed accumulation of GB123 in NeuN-positive neurons, GFAP-positive astrocytes, and OX42-positive microglial cells in cerulein-treated mice; magnified view of boxes in *B* and *C* is located on the right. Scale, 50 μm A, 10 μm *B* and *D*.

pancreatitis induced nocifensive behavior, as assessed by time spent in a hunched position, rearing, and activity levels (Fig. 8*C*). K11777 caused a 2.0-fold decrease in this nocifensive behavior ($P < 0.01$ to vehicle). These results are consistent with cathepsins playing a causative role in cerulein-induced pancreatitis and pancreatitis pain in mice and suggest that cathepsin blockade is a novel therapeutic strategy.

Detection of activated cathepsins in the spinal cord of mice with pancreatitis. Nerve injury results in the activation of Cat-S in spinal microglial cells, and Cat-S released from microglial cells mediates the maintenance of neuropathic pain (8, 9). Since pancreatitis pain is comprised of inflammatory and neuropathic components (7, 21), we assessed whether cathepsin activity is altered in the spinal cord of control mice and mice with pancreatitis. After the tenth dose of cerulein, GB123 was injected, and spinal cord (T8–T10) was collected after the final dose of cerulein. Analysis of a 300-μm-deep projection of T9 spinal cord by two-photon microscopy revealed a marked upregulation of GB123 fluorescence in mice with pancreatitis compared with control mice (Fig. 9*A*). GB123 was detected in discrete cells in all laminae of the dorsal horn. Single-photon analysis of 10-μm sections (T8) confirmed increased GB123 signals in discrete cells (Fig. 9*B*). To identify cell types with GB123 signals, sections were stained with antibody markers for neurons (NeuN), astrocytes (glial fibrillary acidic protein, GFAP), and microglial cells (Ox42). This analysis revealed accumulation of GB123 in neurons (Fig. 9*C*) and microglial cells (Fig. 9*E*), but not in astrocytes (Fig. 9*D*) in mice with pancreatitis. However, the GB123 signals were not sufficiently intense to permit identification of the individual cathepsins by electrophoresis. Thus cathepsins are activated in the spinal cord of mice with cerulein-induced pancreatitis.

Secretion of pancreatic cathepsins in patients with chronic pancreatitis. To determine whether the activation of pancreatic cathepsins in the cerulein model recapitulates the human disease, we evaluated cathepsin activity in pancreatic juice from patients with chronic pancreatitis. We obtained pancreatic juice from three patients with chronic pancreatitis undergoing endoscopic retrograde cholangiopancreatography. Samples were pretreated with the HALT protease inhibitor cocktail, K11777, or vehicle and then labeled by incubation with GB123 and analyzed by SDS-PAGE and in-gel fluorescence. GB123-labeled proteins of the expected mass cathepsins between 29–37.5 kDa (Fig. 10*A*). Cat-B, Cat-L, and Cat-S were identified by immunoprecipitation (Fig. 10*B*). The two proteins pulled down by the Cat-B antibody probably represent GB123 labeling of both active double- and single-chain forms of Cat-B (16). GB123 signals were dramatically reduced by HALT and K11777, conforming identification of activated cathepsins. Thus activated Cat-B, Cat-L, and Cat-S are present in pancreatic juice of patients with chronic pancreatitis.

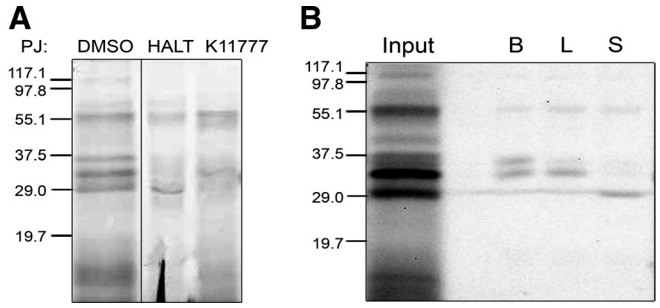

Fig. 10. Detection of activated cathepsins in pancreatic juice (PJ) from patients with chronic pancreatitis. *A*: pancreatic juice from patients (10 μg protein) was bound to GB123. Probe-bound proteases were detected by SDS-PAGE and in-gel fluorescence. Probe-bound proteins with masses corresponding to Cat-B, Cat-L, and Cat-S were detected. HALT and K11777 suppressed signals. GB123 bound a nonspecific protein that was unaffected by protease inhibition. *B*: immunoprecipitation confirmed identification of Cat-B, Cat-L, and Cat-S. Representative gel from $n = 3$ patients.

DISCUSSION

Protease activity is tightly regulated by zymogen processing, enzyme degradation, endogenous inhibitors, and protease trafficking to subcellular or extracellular compartments. Assessment of the contribution of proteases to disease requires the ability to identify and localize active proteases in organs and within cells, which is not possible with use of traditional fluorogenic enzymatic assays that lack selectivity or are unsuitable for localization, or with antibodies that do not discriminate between active and inactive enzymes. By administering a cathepsin-selective ABP to mice with pancreatitis, we demonstrated increased activity of Cat-B, Cat-L, and Cat-S in acinar cells and macrophages of the inflamed pancreas. We also report increased activity of cathepsins within neurons and microglial cells of the spinal cord, a novel finding. A cathepsin inhibitor, which attenuated pancreatitis-induced activation of pancreatic Cat-B, Cat-L, and Cat-S, suppressed pancreatic inflammation and pain. We also identified activated Cat-B, Cat-L, and Cat-S in pancreatic secretions from patients with chronic pancreatitis pain. Our results support an important role for intrapancreatic cathepsins in pancreatic inflammation and pain, and they suggest the possible contribution of centrally acting cathepsins to pancreatic pain. Furthermore, ABPs are a useful tool for the identification of enzymatic mediators that may be predictive biomarkers of disease severity. Similar approaches have revealed activation of cathepsins in cancer (3, 4) and asthma (18).

Inflammation-induced increase in cathepsin activity in the pancreas and spinal cord. Our results show active Cat-S in macrophages and increased activity of Cat-B and Cat-L in acinar cells and macrophages in the pancreas of mice with acute secretagogue-induced pancreatitis. Pancreatic exocrine secretions from patients with chronic pancreatitis pain also contained activated cathepsins B, L, and S. Cat-B activity and immunoreactivity is present in pancreatic juice from patients with hereditary pancreatitis (19), which is consistent with our results. Our findings support the prior report of immunoreactive Cat-L secretion in patients with chronic pancreatitis (36). Active Cat-S has not been previously described in the inflamed pancreas. It is unclear whether pancreatitis-associated increases in cathepsin activity reflect a change in enzyme activity at the level of the individual molecule due to altered bioavailability of protease inhibitors, to increased zymogen synthesis or secretion, or to an influx of protease-containing inflammatory cells. Further experiments are needed to discriminate among these likely possibilities.

By intrathecal administration of GB123 and two-photon imaging, we observed that pancreatitis increases the activity of cathepsins in neurons and microglial cells in the dorsal horn of the spinal cord at levels that receive input from primary spinal

afferent neurons innervating the pancreas. Increased activity of cathepsins in the spinal cord during pancreatitis has not been reported previously. Our findings are consistent with several reports of activation and release of Cat-S from spinal microglial cells following peripheral nerve injury (8, 9). Because of the very small amount of tissue available in the mouse spinal cord, we were unable to specifically identify spinally activated cathepsins by gel electrophoresis. Further studies are required to identify the specific cathepsins that are activated in the spinal cord during pancreatitis and to define their role in pancreatic pain.

Causative role of cathepsins in pancreatitis and pain. Administration of the cathepsin inhibitor K11777 to GB123-treated mice with cerulein pancreatitis inhibited pancreatic Cat-B, Cat-L, and Cat-S. K11777 strongly attenuated all indexes of pancreatic inflammation and suppressed both c-Fos expression by spinal nociceptive neurons and nocifensive behavior. These results confirm a critical causative role for cathepsins in pancreatic inflammation and reveal a new role for cathepsins in pancreatic pain. Since K11777 does not cross the blood-brain barrier (J. McKerrow, personal communication), the analgesic effects of systemic K11777 on pancreatitis pain are presumably due to peripheral inhibition of pancreatic cathepsins.

Mechanisms of cathepsin-induced pancreatic inflammation and pain. One likely pathway by which increased activity of pancreatic cathepsins promotes inflammatory pancreatic pain involves downstream cleavage of trypsinogens and release of trypsin, which we and others have shown causes pancreatic inflammation and pain (13, 35). Most studies of cathepsins in pancreatitis have focused on the mechanisms by which intracellular cathepsins control the premature activation of trypsinogen within acinar cells. Lysosomal Cat-B activates trypsinogen (13, 29, 30, 35), and Cat-L counteracts Cat-B by degrading trypsinogen and trypsin (36). Our findings support reports that Cat-B deletion diminishes cerulein-induced trypsinogen activation and pancreatitis (13) and that Cat-L deletion also reduces the severity of pancreatitis via reduction of necrosis and induction of apoptosis (36). Neither of these studies evaluated pain, a major symptom of pancreatitis.

Cathepsins are also found in peripheral macrophages and prior studies have overlooked the contribution of macrophage-derived cathepsins to the pathogenesis of pancreatitis. Acinar cell injury results in the formation of chemokines and cytokines that attract inflammatory cells to the pancreas, with monocytes and macrophages of particular importance to the pathogenesis of acute pancreatitis (30, 32). Macrophage cathepsins may contribute pancreatitis by upregulating cytokine expression, since Cat-B is required for processing and trafficking of TNF-α (12) and for the maturation and secretion of IL-1β (34).

During chronic inflammation macrophages destroy extracellular matrix by secreting Cat-B, Cat-L, and Cat-S (27). The detection of Cat-B, Cat-L, and Cat-S in human pancreatic juice from patients with chronic pancreatitis indicates secretion of cathepsins, which are therefore available to participate in matrix degradation and possibly inflammatory cell signaling. We were not able to compare cathepsin secretion from patients with chronic pancreatitis to that of controls as pancreatic juice was not available from healthy control subjects. Since pancreatic duct cannulation during endoscopic retrograde cholangiopancreatography carries a significant risk of inducing acute pancreatitis, it was not possible to collect samples from healthy individuals. In pancreatitis, cathepsin-mediated tissue destruction would be predicted to aggravate pancreatitis-associated edema and promote infiltration of inflammatory cells. Interestingly, exocytosis of zymogen granules acidifies the pancreatic duct lumen, particularly when stimulated by cerulein (1), which could enhance cathepsin activity and aggravate inflammation. Extracellular acidification also sensitizes secretagogue-induced zymogen activation and injury (2).

Secreted Cat-S is active at normal extracellular pH and may have widespread extracellular actions (28). Inflammatory mediators including TNF-α, IFN-γ, and NGF, which are abundant during pancreatitis, stimulate Cat-S secretion from macrophages and microglial cells (22). Since Cat-S derives from macrophages and spinal microglial cells (8, 9), peripheral and central neuroimmune mechanisms could mediate its effects on inflammation and pain. Cat-S can activate protease-activated receptor-2 (26, 27), which mediates protease-induced neurogenic inflammation and pain in several tissues, including the pancreas (14, 15, 33). Thus Cat-S secreted from pancreatic macrophages could activate primary spinal afferent neurons to induce neurogenic inflammation and pain. Further studies are required to specifically determine the contribution of Cat-S to pancreatitis and pain.

We conclude that increased activity of Cat-B, Cat-L, and Cat-S in acute pancreatitis is critical for the development of inflammation and pain and that inhibition of these proteases may provide a new approach for the treatment of pancreatitis pain. ABPs can be used to identify activated proteases that cause pancreatic disease. Given the recent advances in fluorescence endoscopy and pancreatoscopy (11, 23), near-infrared ABPs and imaging may provide early diagnosis and mechanistic insights into pancreatic disease.

ACKNOWLEDGMENTS

We thank Dr. Rong Wang and Dr. Ella Jones for assistance with imaging, and Dr. James Ostroff and Dr. James Buxbaum for aid in obtaining human pancreatic juice samples.

GRANTS

This study was supported by Howard Hughes Medical Institute (V. Lyo) and National Institute of Diabetes and Digestive and Kidney Diseases DK3782968, DK46285 (N. W. Bunnett, K. S. Kirkwood), DK43207, and DK57840 (N. W. Bunnett).

DISCLOSURES

No conflicts of interest, financial or otherwise, are declared by the author(s).

AUTHOR CONTRIBUTIONS

Author contributions: V.L., N.W.B., and K.S.K. conception and design of research; V.L., F.C., T.N.K., A.W.W., M.P., D.C., J.C., J.B., and J.O. performed experiments; V.L., F.C., and E.F.G. analyzed data; V.L., M.B., E.F.G., N.W.B., and K.S.K. interpreted results of experiments; V.L. prepared figures; V.L. and K.S.K. drafted manuscript; V.L., N.W.B., and K.S.K. edited and revised manuscript; N.W.B. and K.S.K. approved final version of manuscript.

REFERENCES

1. **Behrendorff N, Foetenmeyer M, Schwiening C, Thorn P.** Protons released during pancreatic acinar cell secretion acidify the lumen and contribute to pancreatitis in mice. *Gastroenterology* 139: 1711–1720.e1–e5, 2010.
2. **Bhoomagoud M, Jung T, Atladottir J, Kolodecik TR, Shugrue C, Chaudhuri A, Thrower EC, Gorelick FS.** Reducing extracellular pH

sensitizes the acinar cell to secretagogue-induced pancreatitis responses in rats. *Gastroenterology* 137: 1083–1092, 2009.
3. **Blum G, Mullins SR, Keren K, Fonovic M, Jedeszko C, Rice MJ, Sloane BF, Bogyo M.** Dynamic imaging of protease activity with fluorescently quenched activity-based probes. *Nat Chem Biol* 1: 203–209, 2005.
4. **Blum G, von Degenfeld G, Merchant MJ, Blau HM, Bogyo M.** Noninvasive optical imaging of cysteine protease activity using fluorescently quenched activity-based probes. *Nat Chem Biol* 3: 668–677, 2007.
5. **Brix K, Dunkhorst A, Mayer K, Jordans S.** Cysteine cathepsins: cellular roadmap to different functions. *Biochimie* 90: 194–207, 2008.
6. **Ceppa E, Cattaruzza F, Lyo V, Amadesi S, Pelayo JC, Poole DP, Vaksman N, Liedtke W, Cohen DM, Grady EF, Bunnett NW, Kirkwood KS.** Transient receptor potential ion channels V4 and A1 contribute to pancreatitis pain in mice. *Am J Physiol Gastrointest Liver Physiol* 299: G556–G571, 2010.
7. **Ceyhan GO, Demir IE, Rauch U, Bergmann F, Müller MW, Büchler MW, Friess H, Schäfer KH.** Pancreatic neuropathy results in "neural remodeling" and altered pancreatic innervation in chronic pancreatitis and pancreatic cancer. *Am J Gastroenterol* 104: 2555–2565, 2009.
8. **Clark AK, Yip PK, Grist J, Gentry C, Staniland AA, Marchand F, Dehvari M, Wotherspoon G, Winter J, Ullah J, Bevan S, Malcangio M.** Inhibition of spinal microglial cathepsin S for the reversal of neuropathic pain. *Proc Natl Acad Sci USA* 104: 10655–10660, 2007.
9. **Clark AK, Yip PK, Malcangio M.** The liberation of fractalkine in the dorsal horn requires microglial cathepsin S. *J Neurosci* 29: 6945–6954, 2009.
10. **Fonovic M, Bogyo M.** Activity based probes for proteases: applications to biomarker discovery, molecular imaging and drug screening. *Curr Pharm Des* 13: 253–261, 2007.
11. **Goetz M, Wang TD.** Molecular imaging in gastrointestinal endoscopy. *Gastroenterology* 138: 828–833.e1, 2010.
12. **Ha SD, Martins A, Khazaie K, Han J, Chan BM, Kim SO.** Cathepsin B is involved in the trafficking of TNF-alpha-containing vesicles to the plasma membrane in macrophages. *J Immunol* 181: 690–697, 2008.
13. **Halangk W, Lerch MM, Brandt-Nedelev B, Roth W, Ruthenbuerger M, Reinheckel T, Domschke W, Lippert H, Peters C, Deussing J.** Role of cathepsin B in intracellular trypsinogen activation and the onset of acute pancreatitis. *J Clin Invest* 106: 773–781, 2000.
14. **Hoogerwerf WA, Shenoy M, Winston JH, Xiao SY, He Z, Pasricha PJ.** Trypsin mediates nociception via the proteinase-activated receptor 2: a potentially novel role in pancreatic pain. *Gastroenterology* 127: 883–891, 2004.
15. **Hoogerwerf WA, Zou L, Shenoy M, Sun D, Micci MA, Lee-Hellmich H, Xiao SY, Winston JH, Pasricha PJ.** The proteinase-activated receptor 2 is involved in nociception. *J Neurosci* 21: 9036–9042, 2001.
16. **Ishidoh K, Kominami E.** Processing and activation of lysosomal proteinases. *Biol Chem* 383: 1827–1831, 2002.
17. **Jacobsen W, Christians U, Benet LZ.** In vitro evaluation of the disposition of a novel cysteine protease inhibitor. *Drug Metab Dispos* 28: 1343–1351, 2000.
18. **Korideck H, Peterson JD.** Noninvasive quantitative tomography of the therapeutic response to dexamethasone in ovalbumin-induced murine asthma. *J Pharmacol Exp Ther* 329: 882–889, 2009.
19. **Kukor Z, Mayerle J, Krüger B, Tóth M, Steed PM, Halangk W, Lerch MM, Sahin-Tóth M.** Presence of cathepsin B in the human pancreatic secretory pathway and its role in trypsinogen activation during hereditary pancreatitis. *J Biol Chem* 277: 21389–21396, 2002.
20. **Laird JM, Martinez-Caro L, Garcia-Nicas E, Cervero F.** A new model of visceral pain and referred hyperalgesia in the mouse. *Pain* 92: 335–342, 2001.
21. **Liddle RA, Nathan JD.** Neurogenic inflammation and pancreatitis. *Pancreatology* 4: 551–559; discussion 559–560, 2004.
22. **Liuzzo JP, Petanceska SS, Devi LA.** Neurotrophic factors regulate cathepsin S in macrophages and microglia: a role in the degradation of myelin basic protein and amyloid beta peptide. *Mol Med* 5: 334–343, 1999.
23. **Meining A, Phillip V, Gaa J, Prinz C, Schmid RM.** Pancreaticoscopy with miniprobe-based confocal laser-scanning microscopy of an intraductal papillary mucinous neoplasm (with video). *Gastrointest Endosc* 69: 1178–1180, 2009.
24. **Nguyen QT, Tsai PS, Kleinfeld D.** MPScope: a versatile software suite for multiphoton microscopy. *J Neurosci Methods* 156: 351–359, 2006.
25. **Petanceska S, Canoll P, Devi LA.** Expression of rat cathepsin S in phagocytic cells. *J Biol Chem* 271: 4403–4409, 1996.
26. **Reddy VY, Zhang QY, Weiss SJ.** Pericellular mobilization of the tissue-destructive cysteine proteinases, cathepsins B, L, and S, by human monocyte-derived macrophages. *Proc Natl Acad Sci USA* 92: 3849–3853, 1995.
27. **Reddy VB, Shimada SG, Sikand P, Lamotte RH, Lerner EA.** Cathepsin S elicits itch and signals via protease-activated receptors. *J Invest Dermatol* 130: 1468–1470, 2010.
28. **Reiser J, Adair B, Reinheckel T.** Specialized roles for cysteine cathepsins in health and disease. *J Clin Invest* 120: 3421–3431, 2010.
29. **Saluja AK, Donovan EA, Yamanaka K, Yamaguchi Y, Hofbauer B, Steer ML.** Cerulein-induced in vitro activation of trypsinogen in rat pancreatic acini is mediated by cathepsin B. *Gastroenterology* 113: 304–310, 1997.
30. **Saluja AK, Lerch MM, Phillips PA, Dudeja V.** Why does pancreatic overstimulation cause pancreatitis? *Annu Rev Physiol* 69: 249–269, 2007.
31. **Sevcik MA, Jonas BM, Lindsay TH, Halvorson KG, Ghilardi JR, Kuskowski MA, Mukherjee P, Maggio JE, Mantyh PW.** Endogenous opioids inhibit early-stage pancreatic pain in a mouse model of pancreatic cancer. *Gastroenterology* 131: 900–910, 2006.
32. **Shrivastava P, Bhatia M.** Essential role of monocytes and macrophages in the progression of acute pancreatitis. *World J Gastroenterol* 16: 3995–4002, 2010.
33. **Steinhoff M, Vergnolle N, Young SH, Tognetto M, Amadesi S, Ennes HS, Trevisani M, Hollenberg MD, Wallace JL, Caughey GH, Mitchell SE, Williams LM, Geppetti P, Mayer EA, Bunnett NW.** Agonists of proteinase-activated receptor 2 induce inflammation by a neurogenic mechanism. *Nat Med* 6: 151–158, 2000.
34. **Terada K, Yamada J, Hayashi Y, Wu Z, Uchiyama Y, Peters C, Nakanishi H.** Involvement of cathepsin B in the processing and secretion of interleukin-1beta in chromogranin A-stimulated microglia. *Glia* 58: 114–124, 2010.
35. **Van Acker GJ, Saluja AK, Bhagat L, Singh VP, Song AM, Steer ML.** Cathepsin B inhibition prevents trypsinogen activation and reduces pancreatitis severity. *Am J Physiol Gastrointest Liver Physiol* 283: G794–G800, 2002.
36. **Wartmann T, Mayerle J, Kähne T, Sahin-Tóth M, Ruthenbürger M, Matthias R, Kruse A, Reinheckel T, Peters C, Weiss FU, Sendler M, Lippert H, Schulz HU, Aghdassi A, Dummer A, Teller S, Halangk W, Lerch MM.** Cathepsin L inactivates human trypsinogen, whereas cathepsin L-deletion reduces the severity of pancreatitis in mice. *Gastroenterology* 138: 726–737, 2010.